Minerals Engineering 232 (2025) 109552

Contents lists available at ScienceDirect

Minerals Engineering

journal homepage: www.elsevier.com/locate/mineng

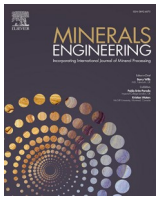

High pressure dewatering rolls Mark-II: A novel dewatering technology for mineral tailings

Sajid Hassan *, Raul Cavalida, Nilanka I.K. Ekanayake, Peter J. Scales, Robin J. Batterham, Anthony D. Stickland

ARC Centre of Excellence for Enabling Eco-Efficient Beneficiation of Minerals, Department of Chemical Engineering, The University of Melbourne, Victoria 3010, Australia

ARTICLE INFO

Keywords:
Filtration
Dewatering
Shear
Compression
High pressure
Rollers

ABSTRACT

High Pressure Dewatering Rolls (HPDR) is a continuous, high pressure, cloth-less filter designed to improve solid–liquid separation. The Mark-I prototype demonstrated cake solid concentrations comparable to those of conventional filter presses during trials with various industrial suspensions. A further development (HPDR Mk-II) is described here. It is designed for mineral tailings, features a larger filtration area, improved handling of fine particles using 30 μm wedge wires as the filter surface, and the potential for cost reductions in achieving low moisture content.

This study overviews the design, proof of concept (phase 1) and safe and continuous steady state operation (phase 2) of the device. Phase 1 demonstrated operation using both flocculated and non-flocculated copper tailings (D[3,2] = 5.84 μm) and phase 2 showcases operation in runs up to one hour with nickel tailings (D[3,2] = 9.33 μm) under varying conditions. Thorough material characterisation of the tailings was conducted for benchmarking purposes. The HPDR achieved filter cake moisture contents of 83.1 wt% for copper and 87.9 wt% for nickel tailings, with a maximum specific solids throughput of 302 kg/m^2.hr for nickel and 73 kg/m^2.hr for copper. The cake moisture and specific throughput were comparable to or better than filter press performance, but with the advantages of continuous, cloth-less operation.

1. Introduction

1.1. Tailings dewatering

Mineral processing often uses solid–liquid separation to recover water for reuse and increase solids concentration before placement of tailings in storage facilities. Any unrecovered water at this stage typically constitutes the majority of makeup water required for ore processing. Thickening, the industry standard for solid–liquid separation (Concha, 2014), can meet all geotechnical, safety, and rehabilitation requirements when tailings storage facilities (TSFs) are properly managed. However, improper water management in tailings can lead to catastrophic dam failures (Hamraoui et al., 2024, Williams, 2021, Chen, 2022, Queiroz et al., 2018, Rotta et al., 2020), meaning that relying on thickening alone carries significant risks of human, environmental, and economic loss if a TSF fails.

For fine tailings, thickening must be followed by desiccation to achieve high solids concentrations, which depends on the balance between local rainfall and evaporation (Williams, 2021). In dry regions, desiccation is more effective but results in water loss that could be recycled. Finer particles result in lower equilibrium solids concentrations due to a greater inter-particle network strength arising from increased particle–particle interactions (Zhou et al., 2001) and reduced liquid permeability caused by increased fluid drag from more surface area per unit volume. Reducing water use and de-risking tailings storage are key drivers in the industry (International Council on Mining and Metals et al., 2020).

High pressure filtration addresses these needs (Chaedir et al., 2021, Haldar, 2018, Furnell et al., 2022), albeit at higher capital and operating costs. Filter presses effectively remove water from suspensions but are expensive and require significant infrastructure. They operate as a batch process with fixed plate separation, limiting flexibility for different feed types, and suffer from issues like cloth fouling and wear, necessitating routine washing and replacement (Furnell et al., 2022).

* Corresponding author.
E-mail address: hassan.s1@unimelb.edu.au (S. Hassan).

https://doi.org/10.1016/j.mineng.2025.109552
Received 30 January 2025; Received in revised form 30 May 2025; Accepted 18 June 2025

Numerous technologies have been developed to address these challenges. Pressure filters are widely used to produce low moisture filter cakes but require filter cloths, involve high capital or maintenance costs, and are prone to clogging—particularly with fine tailings. Gravity-based methods such as high-rate or high-density thickeners are widely adopted for cost-effective bulk water removal but typically produce low solids output, especially for ultrafine or flocculated suspensions. Paste thickeners and thickened tailings filtration systems offer higher solids concentration but require more energy and operational complexity (Haramkar et al., 2021, Furnell et al., 2022, Adewuyi et al., 2024).

Technologies like decanter centrifuges (Menesklou et al., 2020, Menesklou et al., 2021, Gleiss and Nirschl, 2015, Merkl and Steiger, 2012, Reif et al., 1990, Klug and Schwarz, 2019, Adewuyi et al., 2024) and belt filters (Wakeman, 2007, Illies et al., 2017, Chen et al., 2002, Vaxelaire and Olivier, 2006, Vaxelaire and Olivier, 2014, Klug and Schwarz, 2019), apply both compression and shear to enhance dewatering by disrupting interparticle forces (Hammerich et al., 2020, Höfgen et al., 2020). However, these systems often struggle with highly compressible or fine-grained suspensions, where low permeability and strong interparticle forces dominate (Reichmann and Tomas, 2001, Nguyen et al., 2021, Gauthier and Danforth, 1991, Sung and Turian, 1994, Wang et al., 2014).

Despite continued advances in dewatering equipment, significant research gaps remain in developing continuous, low-maintenance systems capable of handling fine, compressible tailings while achieving high solids recovery. Many existing technologies rely on filter cloths, are prone to fouling, operate in batch mode or lack the pressure capacity needed to overcome strong interparticle forces. Additionally, most systems face challenges in scalability and operational flexibility. The HPDR was specifically developed to address these limitations by providing a continuous, cloth-less filtration platform that integrates high mechanical pressure with the capacity to apply vacuum and shear. This configurational versatility allows it to dewater a broader range of tailings materials than vacuum filters or belt presses alone, particularly those that are otherwise difficult to process using conventional methods.

1.2. High pressure dewatering rolls Mark-I

To address the issues with thickening and filtration, a novel solid–liquid separation device, the High Pressure Dewatering Rolls (HPDR) (Scales et al., 2017a, Scales et al., 2017b, Höfgen et al., 2019) was developed. The HPDR features two semi-permeable rotating metal rolls under vacuum. As the rolls rotate, suspension in the feed chamber is filtered, forming a cake on the roll surfaces. The cake is then compressed as it passes through a small gap (nip) between the rolls under high hydraulic pressure.

The HPDR is a continuous filter with adjustable filtration path length and no filter cloths. The high pressure overcomes the interparticle interactions, achieving high solids concentrations, while the adjustable filtration path length mitigates permeability-limited filtration. Independent roll drives also allow for shear incorporation through asynchronous rotation. Additionally, it is envisaged that larger-scale devices will maintain the same filtration path length at the nip, simplifying scale-up.

The Mark-I (Mk-I) prototype was trialled with various compressible industrial suspensions, including Kraft process paper pulp, paper mill wastewater, calcium carbonate, macroalgae, and alum sludge (Höfgen et al., 2019). It achieved cake solids concentrations comparable to conventional high-pressure filter presses. However, the Mk-I rollers, designed for fibrous suspensions, had 500 μm slots that clogged with fine colloidal particles due to the design of the spacing shims. To address this, wedge wire surfaces with 50 μm gap were retrofitted for fine particle suspension dewatering. Despite this, the retrofitted surfaces failed, leading to a redesign of the device into a Mark-II (Mk-II) version, more suited for fine mineral tailings dewatering.

1.3. Study overview

This study documents the design and feasibility assessment of the HPDR Mk-II at the University of Melbourne. Phase 1 demonstrated the proof of concept using flocculated and non-flocculated copper tailings. However mechanical issues identified during this phase led to modifications to the HPDR Mk-II before moving on to Phase 2. In this phase, nickel tailings were used to evaluate continuous operation exceeding 60 min under various operating conditions. Comprehensive material characterisation, including physical, chemical, dewatering, and geotechnical assessments, was performed on both tailings samples, allowing the performance of the HPDR to be benchmarked against dewatering limits determined through these laboratory based material assessments.

Key operational parameters were tested, including roller speed (0.5 to 8 rpm), feed solids concentration (below and above the gel point), submergence level (partial versus full), hydraulic pressure (0 and 7 MPa), and different operating configurations, such as vacuum drum filter mode and differential shear. These tests aimed to determine the effects of these operating parameters on cake solids concentration and throughput. It was hypothesised that:

- Roller speed: Higher speeds would increase throughput but decrease cake solids concentration. Faster throughput limits dewatering time and results in lower applied pressure at the nip.
- Hydraulic pressure: High hydraulic pressures were expected to increase the cake solids concentration by compressing the cake more effectively at the nip, though the solids throughput should remain unchanged.
- Feed solids concentration: Higher feed concentrations were expected to increase throughput by reducing the amount of water needing to be filtered and may improve cake solids concentration if the compression in the nip is limited by the permeability of the cake, not the compressibility. The HPDR was anticipated to perform similarly to vacuum drum filters (Huttunen et al., 2019, Huttunen et al., 2017, Simpson, 1964, Svarovsky, 2001), where higher feed concentration at a fixed roller speed increase both final solids concentration and throughput (Stickland et al., 2011).
- Submersion level: Partial submersion, combined with appropriate vacuum pressure, was hypothesised to enhance dewatering (over compression alone) for materials with low breakthrough pressure by enabling partial desaturation of the cake (Stickland et al., 2011). This would improve cake solids concentration. However, full submersion was expected to yield higher solids throughput due to a greater filtration area.
- Differential shear: Asynchronous roller speeds, introducing shear forces, were hypothesised to improve dewatering by disrupting the particle network structure within the filter cake. This would result in higher cake solids concentration at the same throughput. This ability to incorporate shear effects provides the HPDR a distinct advantage over traditional cavity filtration methods, where shear is neither present nor controllable.

In summary, this study aimed to demonstrate continuous HPDR operation for fine mineral tailings and to investigate the effects of roller speed, feed concentration, submersion level, hydraulic pressure, and shear on HPDR performance.

2. High pressure dewatering rolls (HPDR) Mark-II

2.1. Overview

The HPDR Mk-II prototype, designed and manufactured at the University of Melbourne, addresses the limitations of the Mk-I device by increasing the effective filtration area and enabling finer particle filtration. The Mk-II offers four times the filtration area, with rollers

almost surrounded by suspension instead of only about a quarter of the roll covered, allowing the vacuum system to act over most of the circumference and simplifying the vacuum application. The design incorporates wedge wire cylinders with 30 μm gaps, with one roller fixed and the other floating via a pivot point attached to the bottom of the frame, as shown in Fig. 1.

2.2. Features

Overall Design: Fig. 1 (a) shows a CAD schematic of the HPDR Mk-II. The rollers are housed separately and connected to motors via timing pulleys and rubber belts. The left roller moves freely via a pivot, while the right is fixed, with hydraulic pressure setting the gap. Material is fed from the top, partially or completely filling the volume around the rollers. Cake is formed on the surface of the rollers due to vacuum pressure until both cakes meet at the nip point and are compressed. The dewatered cake is scraped off, collected in a bin, and filtrate is removed from the rollers via the vacuum filtrate line. Adjusting roller speed, hydraulic pressure and fill level allows the system to process various feed types and particle sizes. A level sensor can maintain consistent suspension levels, and filtrate and cake are monitored via balances in the vacuum chamber and product bin. The control cabinet houses a programmable logic controller with continuous data logging.

Motors: The HPDR uses two WEG 1.1 kW 4-pole IP55 B5 electric motors, each with a CFW500 IP20 variable speed drive. Roller speeds range from 0.2 to 8.0 rpm, depending on the timing belt and pulley configuration. Rotary encoders monitor the rotation in real-time.

Hydraulic Cylinders with Accumulators: Two Parker series 3L medium-duty hydraulic cylinders apply pressure to the rollers, with a maximum hydraulic pressure of 13.1 MPa. The floating roller pivots depending on the thickness and strength of the cake it is compressing, controlled by hydraulic pressure, while accumulators absorb shocks from larger particles. Linear encoders monitor the roller gap in real time.

Wedge Wire, Semi-permeable Rollers, and Filtrate Collection: The wedge wire cylinders (Trislot NV) with 30 μm gaps are mounted on permeable rollers, designed to distribute pressure evenly and prevent wedge wire failure. A patent (Stickland et al., 2024) has been filed disclosing the design of the rolls and mounting of the wedge wire to enable fine particle filtration, with the key invention describing how to mount the wedge wire screen without the compressive pressure breaking the welds between the triangular wire and its supporting bars. The wedge wire screens are 200 mm in length and 215 mm in diameter. Filtrate passes through the wedge wire and then through spiral drills in the rollers to a 50 L vacuum chamber connected to a rotary pump (Edwards E1M18).

3. Materials and methods

3.1. Material

Copper and nickel tailings were sourced from operating mine sites of BHP Pty Ltd. A sample of 250 kg of the cyclone overflow of a copper tailings slurry with 43.9 wt% solids was received from an overseas site. Nickel tailings from an Australian mine site, received in two IBCs, were

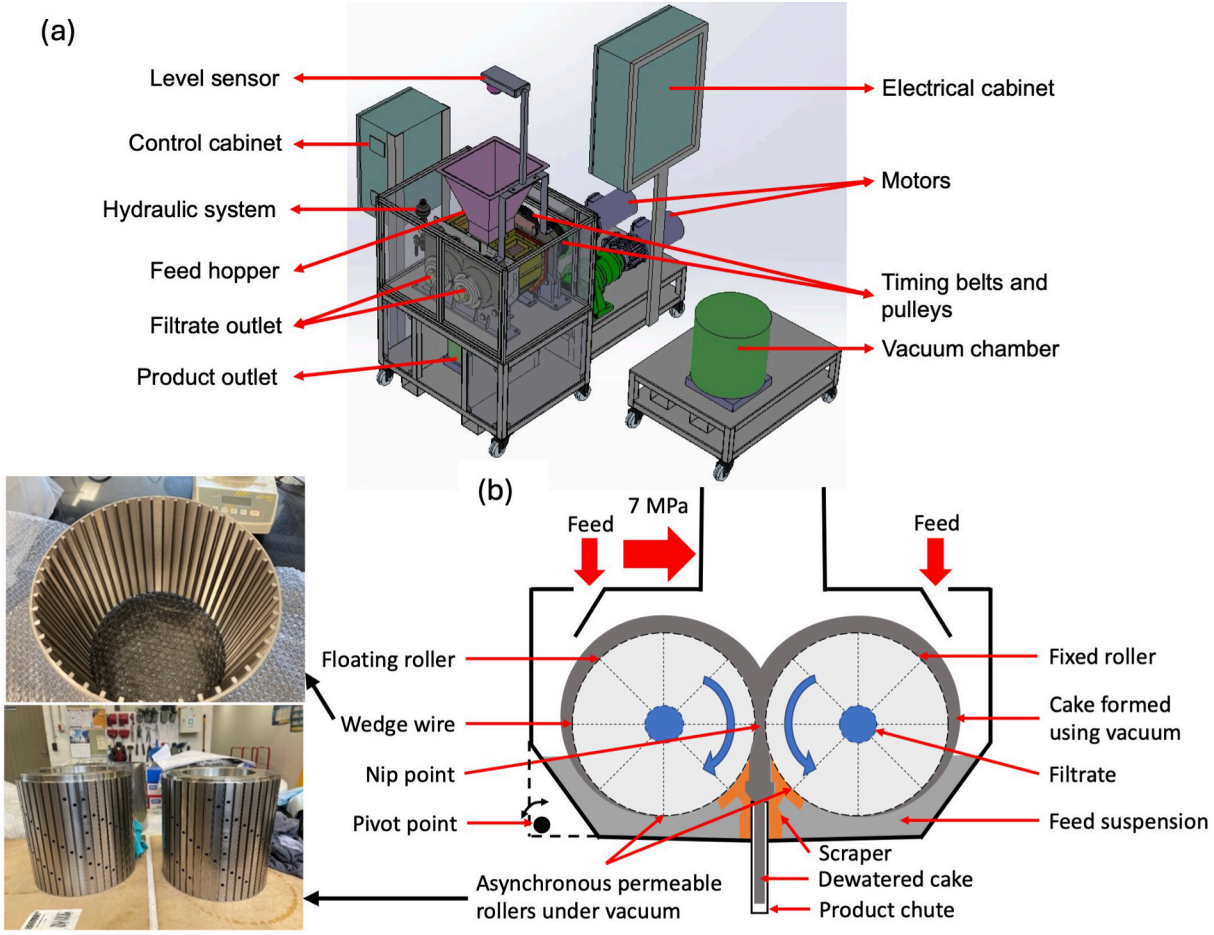

Fig. 1. (a) CAD schematic and (b) internal design of the HPDR Mk-II. The system features two semi-permeable rollers equipped with a hydraulic and vacuum system for effective suspension dewatering. 30 μm wedge wires slide on top of the permeable rollers to facilitate fine particle filtration. Material can be fed through the hopper (a) or from sides of the top (b).

diluted upon receipt and transferred to 205 L steel drums, homogenised by mixing with both an overhead drum mixer and a handheld mixer. They were prepared at different solids concentrations: Drum 1 at 68.5 wt %, and Drums 2 and 3 at approximately 58.0 wt%, representing concentrations above and below the gel point.

3.2. Flocculation

The copper tailings were diluted to 8 wt% using Melbourne tap water to simulate thickener feed. The pH of the water was adjusted to 10.1 using slaked lime to match the operating pH of the actual plant. A high molecular weight anionic flocculant (confidential), identical to the one used at the mine site, was prepared at 0.03 wt% in Melbourne water without pH adjustment and mixed for 24 h using roller mixers. The optimal dosage was determined through settling tests in 1 L measuring cylinders, with 20 g/t selected for HPDR tests based on the dosage used for the thickener on-site.

3.3. Physical and chemical characterisation

Representative 20 L non-flocculated samples were extracted and homogenised from each drum for material characterisation, with triplicate measurements taken. Dissolved solids in the liquor were measured using vacuum filtration with a 0.22 μm PVDF membrane (Durapore, Merck). Both dissolved and total solids were determined by oven drying at 105 °C for 24 h. Moisture content was calculated on a wet basis (MC_w%) and a dry basis (MC_d%), the latter for geotechnical tests, using the following equations:

$$MC_w\ wt\%\ (wet\ basis) = \left(\frac{m_{wet} - m_{dry}}{m_{wet}}\right) \times 100 \quad (1)$$

$$MC_d\ wt\%\ (dry\ basis) = \left(\frac{m_{wet} - m_{dry}}{m_{dry}}\right) \times 100 \quad (2)$$

Density was measured using a pycnometer, zeta potential with a Zetasizer Nano ZS (Malvern), and pH and electrical conductivity with a Hach HQ40d meter. Particle size was analysed using laser diffraction (Mastersizer 3000, Malvern). Refractive and absorption indexes were set at 1.55 and 0.1, respectively, to maintain a weighted residual under 1 %. Scanning electron microscope (SEM) images of the copper tailings were captured with a Hitachi FlexSEM 1000 SEM, since the copper tailings had considerable fine particles. Wet nickel tailings were imaged using an Olympus BX51 microscope, which was sufficient for coarser particles.

3.4. Dewatering characterisation

3.4.1. Compressibility and permeability

To achieve high solids concentrations, the applied force must exceed the network strength of the suspension, represented by the compressive yield stress, $P_y(\phi)$, due to cohesive interparticle forces. $P_y(\phi)$ represents the equilibrium dewatering limit for a given applied stress and was first introduced through the theoretical framework of Buscall and White (1987). The framework also defined the gel point of a suspension, ϕ_g, as the minimum solids volume fraction at which a self-supporting network forms, i.e. $P_y\left(\phi_g\right) = 0$. Permeability is affected by the hydrodynamic interactions, quantified as the hindered settling function, $R(\phi)$, which is inversely proportional to Darcian permeability. $P_y(\phi)$ and $R(\phi)$ were determined through stepped pressure filtration and batch sedimentation tests. For sedimentation (Lester et al., 2005), suspensions were diluted below the gel point, and height versus time data were recorded. Stepped pressure filtration (piston-driven) (de Kretser et al., 2001, Usher et al., 2001, Green et al., 1998) with a 0.22 μm PVDF membrane (Durapore, Merck) was utilised at applied pressures of 20, 40, 80, 150, 300, 600 and 1000 kPa for suspensions above the gel point, with dewaterability curves fitted according to Usher et al. (2013).

3.4.2. Shear yield stress

Shear yield stress was measured using the vane-in-a-large-cup method (Fisher et al., 2007) with a Haake VT500 rheometer. Suspensions were mixed for 2 min with a high-speed overhead mixer, then lightly tapped for 30 s to remove air bubbles. After a 2-minute wait, the vane was rotated at 0.2 rpm to record the peak stress.

3.4.3. Breakthrough pressure

In air-driven dewatering such as vacuum filtration, the capillary pressure, P_{cap}, at the air–liquid interface increases with consolidation until reaching the maximum capillary pressure, P_{cap}^{max}, beyond which desaturation occurs. The breakthrough pressure, P_b, is the point where cake consolidation ends, and desaturation begins. This was measured using air-driven filtration, and the corresponding solids concentration at which breakthrough occurs is termed the critical capillary concentration, x_{cap} (Stickland et al., 2014). A stepped pressure method was used to initially narrow the range, followed by single pressure tests within a 2.5 kPa range to find P_b.

3.5. HPDR tests

3.5.1. HPDR configuration

Phase 1: Both flocculated and non-flocculated copper tailings were tested using the HPDR setup shown in Exp 01 of Fig. 2. The rollers were fully submerged in the suspension to ensure uniform cake formation and consistent vacuum pressure. Due to limited sample availability and to avoid recycling material, only one roller speed was used, allowing the system to reach steady state before measuring cake solids concentration. In this phase, material was fed through the hopper at the top of the HPDR. Additional tests on copper tailings using a different HPDR configuration (top partially submerged) and varying roller speeds were detailed in Hassan et al. (2023).

Phase 2: With more nickel tailings available, various HPDR configurations were explored to assess the full capabilities of the device. Fig. 2 shows the different configurations used. Exp 03 involved only the fixed roller connected to the vacuum, functioning as a vacuum drum filter with no hydraulic pressure and only partial submersion of the roller. This arrangement has no compression or shear on the cake. Exp 04 was similar but used both rollers without hydraulic pressure; the floating roller could open when cakes from both sides met. Exp 02 was like Exp 04 but included 7 MPa of hydraulic pressure, while Exp 01 mirrored Exp 02 but with full submersion of the material. Exp 05 and Exp 06, which explored the effects of feed concentration and shear, followed the same configuration as Exp 02.

3.5.2. Feed Preparation

To prepare the flocculated copper tailings, the slurry was diluted to 8 wt% using Melbourne tap water adjusted to pH 10.1 with slaked lime. An anionic flocculant was added to 50 L buckets at a dosage of 20 g/t. The slurry was mixed for 30 s at high speed to disperse the flocculant, followed by 3 min of slow mixing to ensure uniform floc formation. After settling, free water was decanted, additional water was evaporated using a fan to achieve 52–56 wt% solids, mimicking the thickener underflow concentration on site. This material was the feed to the HPDR.

For non-flocculated copper tailings, the sample was decanted and evaporated using a fan to the desired solids concentration without pH adjustment.

In Phase 1, the material was fed through the hopper, but initial modelling results indicated cake erosion. Therefore, holes in the side of the top with 45-degree splash plates were used in Phase 2 to guide the material around the rollers. The material was manually fed into the HPDR to maintain desired levels.

3.5.3. Experimental parameters

Phase 1: HPDR tests for copper tailings used the parameters shown

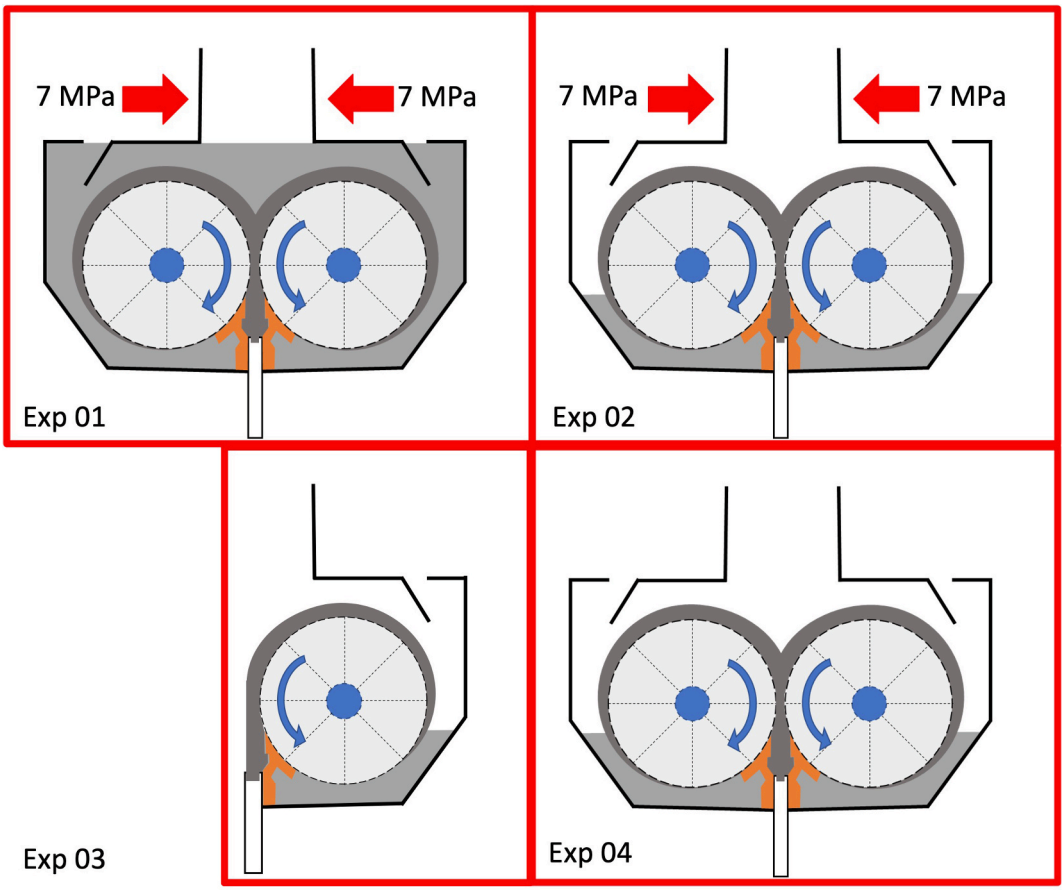

Fig. 2. HPDR configurations for testing nickel tailings. The copper tailings were tested using the Exp 01 configuration. Hydraulic pressure of 7 MPa was applied in Exp 01 and Exp 02, while Exp 03 and Exp 04 were operated without hydraulic pressure.

in Table 1. The HPDR was filled with suspension such that the rollers were completely submerged (see configuration Exp 01 in Fig. 2). Hydraulic pressure was set at approximately 7 MPa, with a minimum roller gap of 0.2 mm. Vacuum pressure was initially set at −90 kPa, and a constant roller speed of 0.44 rpm was applied to reach a steady state. A flocculant dosage of 20 g/t was used for flocculated samples.

Phase 2: Six experiments were conducted with nickel tailings, summarised in Table 2. The first four tests (Exp 01–04) were performed with an average initial concentration of 58.0 wt%, below the gel point of 63.9 wt%, to explore different HPDR configurations. Exp 05 had a feed concentration of 68.8 wt% and used partial submersion with 7 MPa hydraulic pressure for varying speeds. Exp 05 and Exp 06 also had differential roller speeds (0–20 %) at an average of 0.5 rpm.

3.5.4. *Throughput calculations*

Three different methods were employed to calculate the solids throughput, Q_s, expressed in units of kg/m^2.hr. In all methods, the solids throughput is normalised by the total filtration area, A (in m^2), of the wedge wire cylinder. The parameter x denotes solids concentration on a weight/weight basis (w/w), m represents mass (in kg), and t denotes time (in hours).

Ideally, these methods should yield similar results under optimal conditions; however, mass balance closure was not possible for the parameters measured such that each method has some shortcomings and any discrepancies between them can provide valuable insights into the actual performance of the HPDR system such as product chute clogging, cake slipping, and material floating on top of the rollers. These methods are as follows:

Cake Mass: This method calculates Q_s using the direct measurement of the mass of cake collected over a known time interval, multiplied by

Table 2
HPDR test parameters for nickel tailings.

Exp No.	Submerge level	HPDR	Feed conc (wt%)	Speed (rpm)	Shear	Hydraulic pressure (MPa)
01	Full	1	58.0	8 to 0.5	No	7
02	Partial	1	58.0	8 to 0.5	No	7
03	Partial	0.5	58.0	8 to 0.5	No	0
04	Partial	1	58.0	8 to 0.5	No	0
05	Partial	1	68.8	8 to 0.5	0.5 rpm (0 to 20 %)	7
06	Partial	1	59.1	0.5 rpm	0.5 rpm (0 to 20 %)	7

Table 1
HPDR test parameters for copper tailings (flocculated and non-flocculated).

Feed type	Feed solids (wt%)	Submerge type	Roller speed (rpm)	Hydraulic pressure (MPa)	Flocculant dosage (g/t)
Non-flocculated	55.0	Fully	0.44	7.0	0
Flocculated	54.3	Fully	0.44	7.0	20

the average cake solids concentration during steady-state operation:

$$Q_{s1} = \left(\frac{m_{c1} - m_{c2}}{t_2 - t_1}\right) \times x_c \times \frac{1}{A} \quad (3)$$

where m_{c1} and m_{c2} are the masses of cake collected at times t_1 and t_2, respectively, x_c is the average cake solids concentration, and A is the total filtration area.

Roller Gap and Speed: This approach calculates the solids throughput based on the average roller speed, average roller gap, roller dimensions, and average cake solids concentration:

$$Q_{s2} = (S \times 2\pi \times r) \times gL \times \rho_c x_c \times \frac{1}{A} \quad (4)$$

where S is the roller speed in rotations per hour, r is the roller radius, g is the roller gap, L is the roller length, ρ_c is the cake density, x_c is the average cake solids concentration, and A is the total filtration area.

Filtrate: This method calculates the solids throughput from the measured mass of filtrate collected over a time interval, combined with the overall and component mass balances:

$$Q_{s3} = x_c \times \left(\frac{x_0 - x_f}{x_c - x_0}\right) \times \left(\frac{m_{f2} - m_{f1}}{t_2 - t_1}\right) \times \frac{1}{A} \quad (5)$$

where, m_{f1} and m_{f2} are the masses of filtrate collected at times t_1 and t_2, x_0 is the initial solids concentration in the feed, x_f is the average filtrate solids concentration, x_c is the average cake solids concentration, and A is the total filtration area.

3.5.5. Shear difference and rate

To induce shear effects, one roller is rotated faster while the other is rotated slower, maintaining a constant average rotation speed for comparison with no shear. The shear difference is defined as:

$$\textit{Shear difference}(\%) = \frac{\omega_1 - \omega_2}{\frac{\omega_1 + \omega_2}{2}} \times 100 \quad (6)$$

The average shear rate, $\dot{\gamma}$, across the gap between the rollers, g, is defined as (Höfgen et al., 2019):

$$\dot{\gamma} = \frac{\omega_1 r_1 - \omega_2 r_2}{g} \quad (7)$$

In these equations, ω represents the angular velocity (rad/s), and r represents the radius of the rollers.

3.6. Geotechnical tests

Unconfined Compressive Strength (UCS) tests followed ASTM D2166 to measure maximum axial compressive stress under zero confining pressure of the HPDR product. Two 900 g samples were tested at displacement rates of 1.5 mm/min and 2 mm/min. Loading continued until the load decreased with strain or until 15 % strain was reached, with failure assumed at 15 % strain if no maximum load was observed, as per the standard. The liquid limit (LL) was determined using the one-point Casagrande method and cone liquid limit tests per AS1289.3.1.2 and AS1289.3.9.1. The plastic limit (PL) and plasticity index were measured using AS1289.3.2.1 and AS1289.3.3.1 methods.

4. Results and Discussion

4.1. Physical and chemical characterisation

The as-received copper tailings had a pH of 6.8, a zeta potential of −19.4 mV, and an electrical conductivity of 7.3 mS/cm. Dissolved solids in the liquor were 0.6 wt%. The densities of liquor and solids were 999 kg/m^3 and 3028 kg/m^3, respectively. For nickel tailings, drum 1 contained solids above the gel point at 68.5 wt%, while drums 2 and 3 were below the gel point at 58.0 wt%. The particles in the nickel tailings had a zeta potential of −3.1 mV, a pH of 6.6, and an electrical conductivity of 14.4 mS/cm. Dissolved solids were 1.1 wt%. Liquor and solids densities were 1007 kg/m^3 and 2952 kg/m^3, respectively. The low zeta potential of the nickel tailings indicates low electrostatic repulsion between particles, suggesting a potential for spontaneous coagulation.

4.1.1. Particle size distribution

Particle size and shape have critical roles in dewatering, affecting permeability, compressibility, and HPDR filtrate composition, especially during initial cake build-up, where fines can pass through the filter media surface. Copper tailings samples from three different buckets exhibited consistent particle size distribution (PSD). Similarly, nickel tailings from the three drums showed uniform PSD after mixing. Table 3 provides a comprehensive summary. The copper tailings were finer than the nickel tailings. The Sauter mean diameter, D[3,2], of the nickel tailings was 9.33 μm, compared to 5.84 μm for the copper tailings. The nickel tailings, with a d_{50} of 43.2 μm, were significantly coarser than the copper tailings (d_{50} = 11.8 μm), potentially improving dewatering efficiency and also fewer particles would pass through the 30 μm filter gap during initial cake build-up, assuming a similar state of flocculation. Note that the specific surface area given in Table 3 was calculated from the size distribution and solids density, not independently measured.

4.1.2. Microstructure

SEM images of the copper tailings (Fig. 3 (a)) show a significant amount of clay (platy) material, much of it either on the surface of particles or embedded in composite particles. The aspect ratio of the platy material is predominately < 50, suggesting that it has not swollen and broken up into individual clay platelets, as might occur with swelling 2:1 clays such as montmorillonite. There is a range of particles of order 5 to 10 μm (long axis) and 0.5 to 2 μm (short axis), suggesting that the average aspect ratio is of order 10.

Microscopic images of the nickel tailings (Fig. 3 (b)) show a heterogeneous composition with particles up to 100 μm exhibiting a predominantly non-spherical angular morphology.

4.2. Dewatering characterisation

4.2.1. Compressive and shear yield Stress, breakthrough Pressure, and desaturation

This study compares the dewatering characteristics of nickel tailings with flocculated and non-flocculated copper tailings. Compressive yield stress and hindered settling data were obtained from stepped pressure filtration at higher solid concentrations and batch sedimentation tests at lower concentrations.

Fig. 4 shows the compressive and shear yield stress versus solids weight fraction. Results from stepped pressure filtration for all three drum samples of nickel tailings and repeated tests for copper tailings were consistent for compressive yield stress and hindered settling functions.

Flocculated copper tailings exhibited slightly lower solids weight fractions at lower pressures compared to non-flocculated tailings due to the added strength of the flocs. The gel points were 38.5 wt% for flocculated and 40.0 wt% for non-flocculated copper tailings. At higher

Table 3
Particle size distribution summary of as-received copper and nickel tailings.

Parameter	Copper	Nickel
Specific Surface Area (m^2/kg)	1027	643.1
D[3,2] (μm)	5.84	9.33
D[4,3] (μm)	45.9	78.2
d_{10}(μm)	2.41	3.55
d_{50}(μm)	11.8	43.2
d_{90}(μm)	149	207

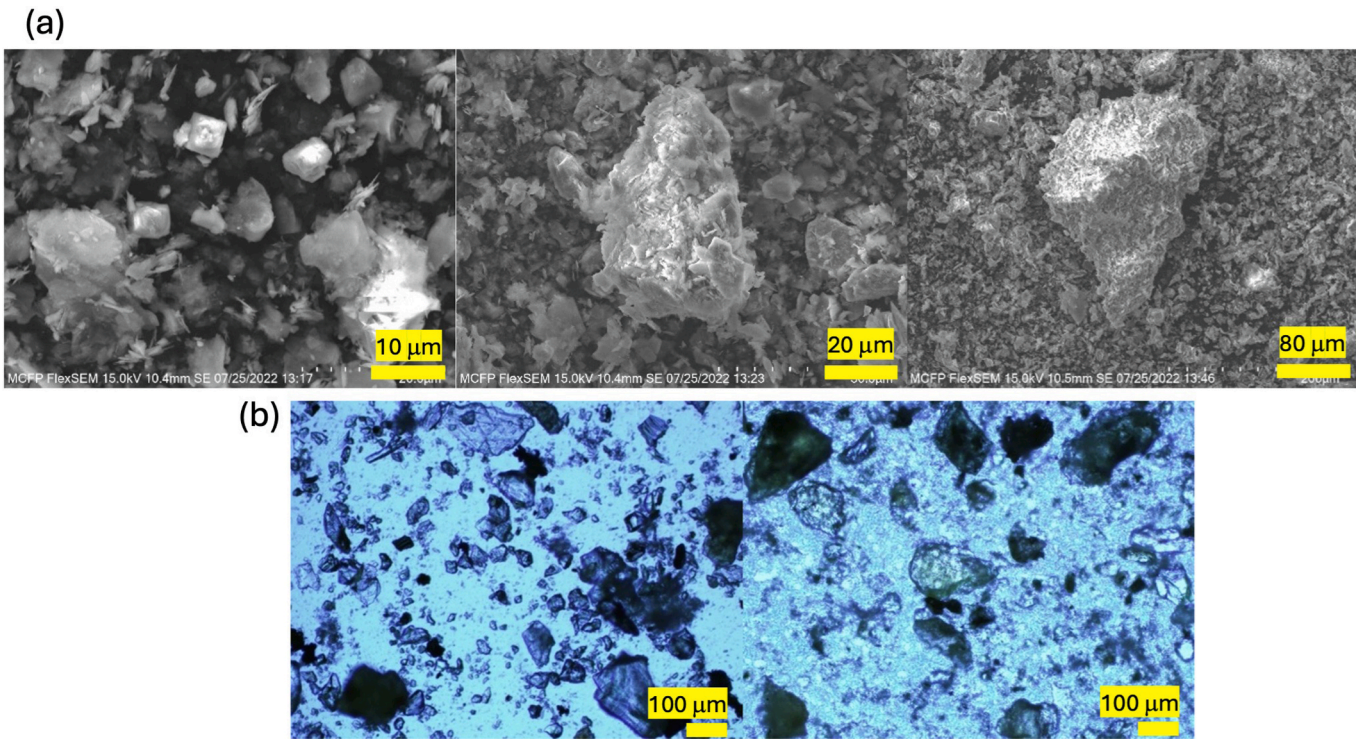

Fig. 3. (a) SEM images of as-received copper tailings and (b) microscopic images of nickel tailings.

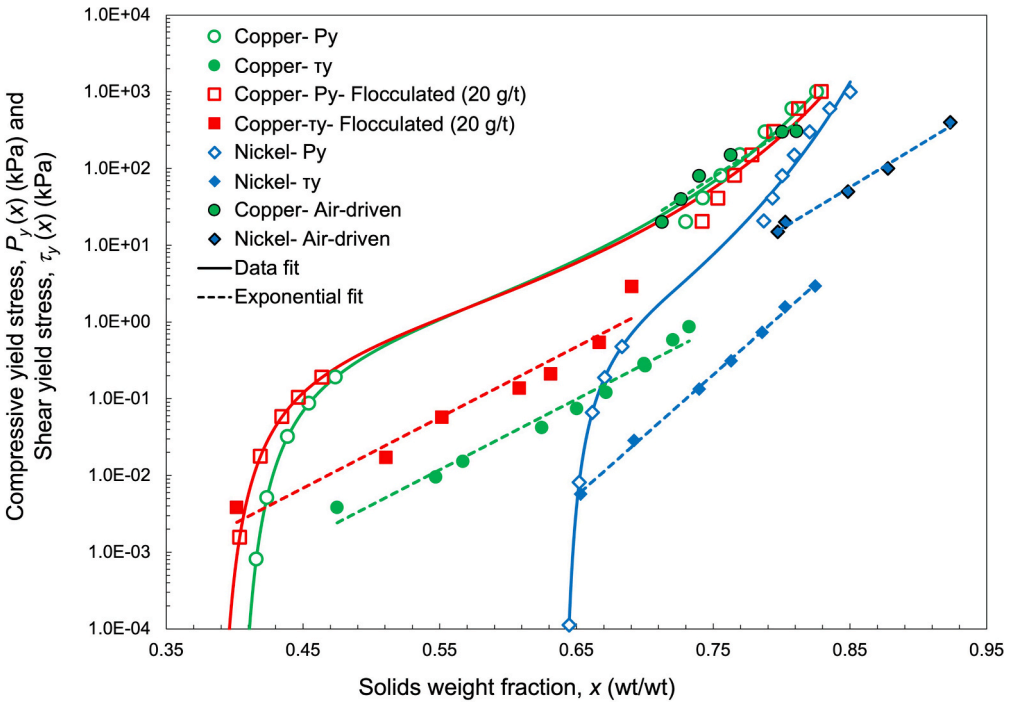

Fig. 4. Compressive and shear yield stress of flocculated copper, non-flocculated copper, and nickel tailings.

pressures, flocculation had minimal effect on compressibility.

The nickel tailings, with coarser particles, show much lower compressive yield stress than the copper tailings, attributed to their lower surface area to volume ratio. The gel point for nickel tailings was 63.9 wt%, significantly higher than for copper tailings, and would therefore be expected to reach higher underflow concentrations in a thickener. The nickel tailings demonstrate better dewatering at all pressures, though the difference narrows at higher concentrations as both tailings approach their compressibility limit. Notably, the logarithmic scale of the y-axis highlights the considerable strength required for even a marginal increase in cake solids concentrations. At 1 MPa pressure, the nickel tailings reach an equilibrium solids concentration of 85.0 wt%, compared to 82.9 wt% for the copper tailings, indicating a slightly better extent of dewatering at high pressures.

Tailings typically exhibit shear thinning behaviour, where viscosity decreases with increasing shear rate due to particle alignment in the

direction of shear and a reduction of the influence of Brownian motion-induced particle aggregation. Both of these factors reduce the resistance to flow (Boger et al., 2006). However, higher particle concentrations increase viscosity due to greater flow resistance. The shear yield stress is up to two orders of magnitude lower for the non-flocculated copper and nickel tailings and up to one order of magnitude lower for flocculated tailings compared to their compressive yield stress (Fig. 4). If one looks at the expected output of a thickener, nominally at a shear yield stress of 20 Pa, flocculated copper tailings would likely result in an underflow solids concentration of around 50 wt%, while nickel tailings would be about 68.5 wt%.

The study underscores the importance of considering both compressive and shear effects in HPDR operations. Utilising varying roller speeds and shear rates above critical thresholds can disrupt particulate networks, reducing compressive yield stress and improving dewatering.

Desaturation effects were also examined using an air-driven filtration rig, revealing breakthrough pressures (P_b) of 302.5 ± 2.5 kPa for the non-flocculated copper and 17.5 kPa for the nickel tailings. Critical capillary concentrations (x_{cap}), the concentration at the point of breakthrough, were 79.1 wt% and 77.8 wt%, respectively. Flocculated copper tailings showed the same P_b value as the non-flocculated tailings. Pressures above these thresholds lead to desaturation as water is replaced by air in the cake pore structure.

The copper tailings required pressures above 302.5 kPa for desaturation, which cannot be achieved with vacuum drum filters or the HPDR. In contrast, nickel tailings are predicted to be desaturated with vacuum drum filters and the HPDR at vacuum pressures below −17.5 kPa. At 100 and 400 kPa air pressures, the nickel tailings reached solid concentrations of 87.8 wt% and 92.3 wt%, respectively. Although vacuum drum filters are limited to 101.3 kPa, a filter press with cake blowing at 400 kPa is expected to show these figures as an upper dewatering limit.

4.2.2. Permeability

The hindered settling behaviour, which is inversely related to permeability, of the nickel tailings was compared to both the flocculated and non-flocculated copper tailings (Fig. 5). The results show that the flocculated copper tailings have higher permeability than the non-flocculated copper tailings at all solid concentrations. At higher concentrations, the permeability of the flocculated copper tailings nearly doubles, suggesting that flocculant use is expected to significantly improve dewatering rates. The nickel tailings exhibit much higher permeability than both types of copper tailings across all solid concentrations. The coarser particles in the nickel tailings reduce surface area and create less fluid-particle resistance, allowing for faster fluid movement. At high solids concentrations, the nickel tailings demonstrate up to 14 times greater permeability than the flocculated copper tailings. As such, the nickel tailings are predicted to dewater more efficiently in the HPDR process, achieving higher throughputs at faster rates as the cake reaches higher concentrations more quickly.

4.3. HPDR raw results

The Programmable Logic Controller (PLC) of the HPDR logs key parameters such as roller gap, hydraulic pressure, roller speed, vacuum pressure, cake mass, and filtrate mass. Fig. 6 presents raw data from a test using the nickel tailings, where both partially submerged rollers rotated at 0.5 rpm without added hydraulic pressure (Exp 04). The first 150 s represent the start-up phase, with the vacuum pump activated, rollers turning, and feed introduced. As cake formation began, vacuum pressure increased, and the mass of the cake and filtrate followed a linear trend between 263 and 563 s, indicating steady-state conditions. During this period, the roller gap averaged 8.8 mm. Hydraulic pressure remained at zero, with minimal fluctuation (±0.08 MPa), while vacuum pressure fluctuated between −30 and −45 kPa, influenced by factors such as feed introduction, cake formation, and air passage after desaturation.

4.4. Phase 1: Non-flocculated and flocculated copper tailings

In industrial applications, flocculants are often added to thickener feeds before tailings undergo further dewatering or storage. However,

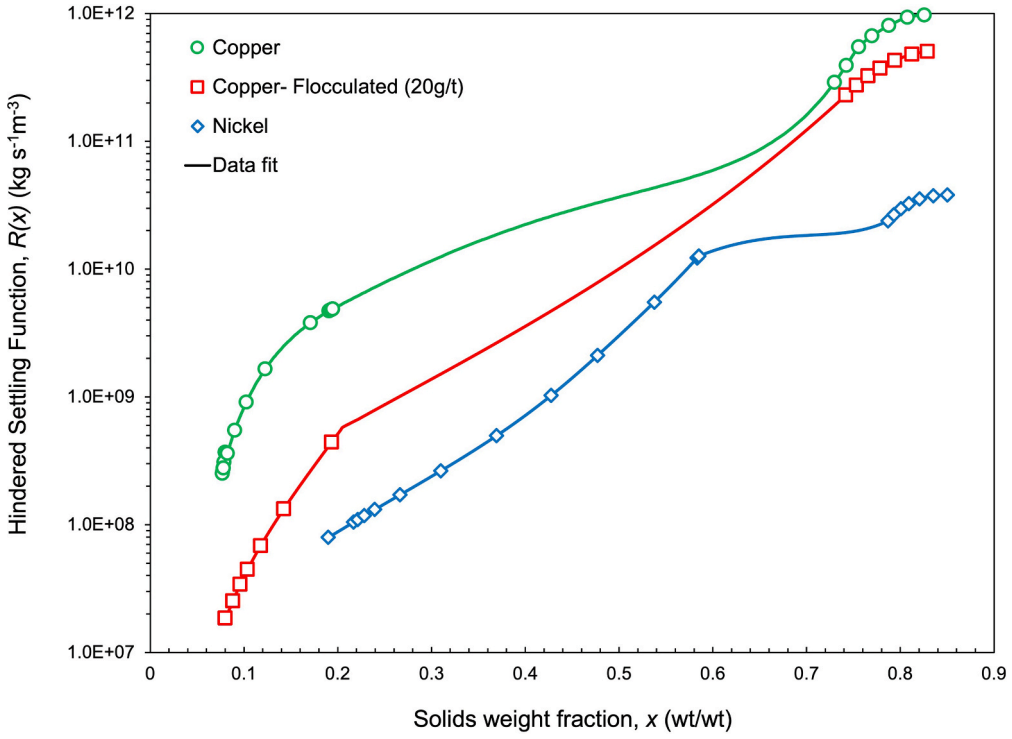

Fig. 5. Hindered settling function of flocculated copper, non-flocculated copper, and nickel tailings.

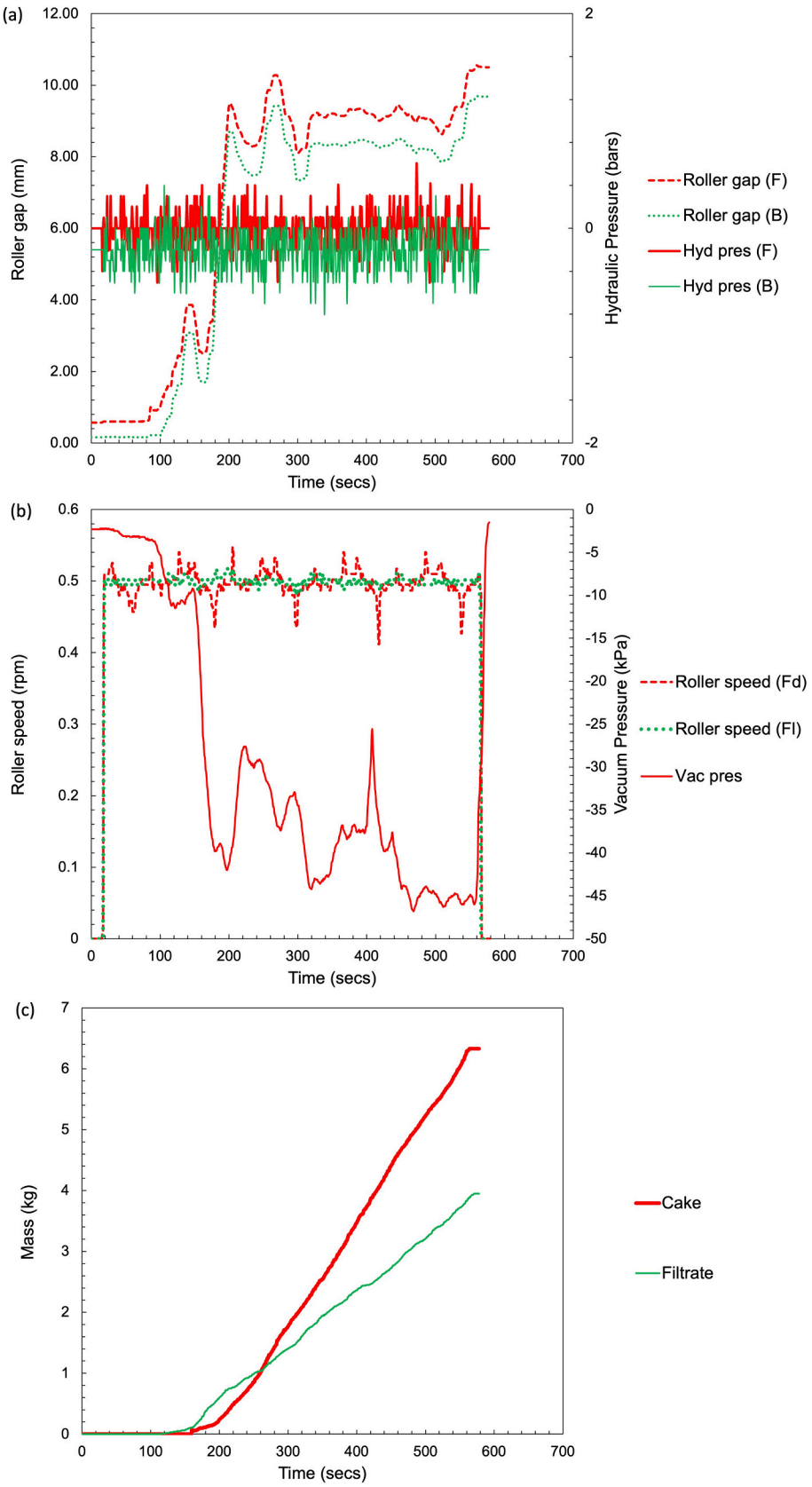

Fig. 6. Raw results from HPDR testing using the nickel tailings (Exp 04). Both rollers were partially submerged and rotated at 0.5 rpm without applying hydraulic pressure. The first 150 s represent the start-up phase. (Key: F = Front, B = Back, Fd = Fixed, Fl = Floating).

shear forces from pumps tend to break down flocs, negating the effectiveness. To demonstrate the HPDR Mk-II for dewatering mineral tailings, two tests were performed using copper tailings, one with flocculant and one without. Key parameters are listed in Table 1. The primary goal was to determine the maximum achievable solids concentration as an indicator of the dewatering performance of the device. Due to limited sample availability, the tests were semi-batch, with tailings fed through the hopper until the rollers were exposed. Although the process was not fully continuous, steady-state filtration was achieved by keeping the rollers fully submerged.

The roller speed was kept low (0.44 rpm) due to limited sample availability, the goal of reaching compressive equilibrium, and a focus on maximising cake solids concentrations. Both tests maintained hydraulic pressure around 7 ± 0.2 MPa, with vacuum pressures stabilising at −40 kPa (non-flocculated) and −50 kPa (flocculated). Initially, most suspension flowed through the nip, but once the rollers were fully submerged, cake buildup began. The initial cake thickness ranged from 1 to 3 mm (Fig. 7 (a)) but, as the run progressed, blockages occurred at the outlet, causing the cake to accumulate and extrude in chunks. It was deduced that the solids concentration of the cake remained unaffected, as there was no dewatering mechanism present beneath the rollers. Notably, the final cake thickness, averaging around 20 mm (depicted in Fig. 7 (b) and (c)), corresponded to the product chute dimensions rather than the roller gap itself. This led to improved product chute design in Phase 2 to help facilitate better cake discharge.

Using 7 MPa of hydraulic pressure, both the non-flocculated and flocculated tests achieved similar maximum cake solids concentrations of 83.0 wt% and 83.1 wt%, indicating that the flocculant had minimal impact on dewatering at higher pressures, as both cakes approached their compressibility limits. These results were similar with the characterisation results for 1 MPa (82.9 wt%) (Fig. 4). Notably, the HPDR cake is compressed at the nip before emerging as a product, but yielding results comparable to characterisation data that allow sufficient time to reach equilibrium. Without feed or operational optimisation, both tests produced cakes with solids concentrations similar to those from other filtration devices, and incorporating shear is expected to further enhance these outcomes.

The roller gap size and speed are critical for throughput. One roller was designed to float, enabling cake to push the rollers apart and enlarge the gap, despite hydraulic pressure aiming to maintain compression. In both test scenarios, the cake displaced the floating roller by 2 to 6 mm.

4.5. Phase 2: Nickel tailings

After the Phase 1 testing, the HPDR was modified to improve the scrapers and product chute to help alleviate cake clogging, to fix the alignment of the drive belts and install timing belts to prevent belt slippage, and to upgrade the sealing to reduce leakage. After the modifications, tests were performed using the nickel tailings to investigate the effect of roller speeds, hydraulic pressures, submersion levels, and HPDR arrangements on cake solids concentration and throughput. An important consideration during this phase of testing was continuous operation and steady-state throughput measurement.

4.5.1. Impact on cake solids concentration

Phase 2 testing of the redesigned HPDR Mk-II provided key insights. The breakthrough pressure for nickel tailings was 17.5 kPa. When operating as a vacuum drum filter (Exp 03) (0.5 HPDR-PS-0 MPa), the average vacuum pressure across all speeds was around −65 kPa, specifically at −63.4 kPa at 0.5 rpm. The predicted maximum solids concentration from characterisation data (Fig. 4) is 85.0 wt%, given that the breakthrough pressure is lower than the vacuum system pressure leading to desaturation. The highest cake solids concentration recorded was 84.9 wt% at 0.5 rpm (Fig. 8 (a)), closely matching predictions. However, the cake concentration decreased with higher roller speeds, falling to 82.3 wt% at 4 rpm and 81.9 wt% at 8 rpm, suggesting that the roller speed exceeded the rate at which the cake could fully desaturate, and the system became what is termed ‘permeability limited’.

In tests imitating dual vacuum drum filters (Exp04) (HPDR-PS-0 MPa), the cake solids concentration remained consistent except at 0.5 rpm, where it increased to 85.9 wt%. In a dual vacuum drum arrangement, cake formation occurs on both rollers. When the cakes converge, the absence of hydraulic pressure allows the floating roller to open more, preventing additional cake compression at the nip point. At 0.5 rpm, the roller gap was around 9 mm, allowing each roller to ideally have a 4.5 mm thick cake. Despite a maximum vacuum pressure of −46.8 kPa, which theoretically results in an 83.8 wt% cake solids concentration, the observed concentration was 85.9 wt%, indicating additional compression at the nip. This discrepancy suggests that both cakes compress against each other when they meet, even though no hydraulic pressure is applied.

The compressive yield stress (Fig. 4) shows that, at 1 MPa, the cake concentration reaches 85.0 wt%. With a vacuum pressure of –32.4 kPa, leading to desaturation, the expected concentration is about 82.3 wt%. At 7 MPa hydraulic pressure (Exp 02) (HPDR-PS-7 MPa) with a vacuum pressure of –32.4 kPa, the partially submerged setup achieved a peak cake solids concentration of 87.9 wt% at 0.5 rpm, indicating a combined effect of compression and desaturation. Despite the expectation of higher solids concentration at 1 rpm due to hydraulic pressure, the concentration remained similar to tests without hydraulic pressure (84.0 wt%). The maximum vacuum pressure of −36.7 kPa in this case, theoretically yielding 82.8 wt%, suggests that lower vacuum pressure may have offset the increased compression effect, resulting in comparable cake concentrations.

At high speeds (8 and 4 rpm), the roller gaps were small (0.25 mm and 0.31 mm, respectively) (Fig. 8 (c)), forming thin cakes that accumulated and floated above the gap (Fig. 9 (a)) as it could not pass through the nip point due to high hydraulic pressures. At 1 rpm, the gap expanded to 2.24 mm, achieving a cake concentration of 84.0 wt% with no solids floating above the nip, but the cake appearing from the product chute was ~ 20 mm thick (Fig. 9 (b)), suggesting the cake at this concentration was sticky and had clogged the product chute. At 0.5 rpm, with a roller gap of 3.94 mm, the concentration increased to 87.9 wt%, with the cake falling as thin sheets (Fig. 9 (c)). In this case, the cake was dryer and did not block the product chute.

In the fully submerged HPDR test (Exp01) (HPDR-FS-7 MPa), no desaturation was expected. Cake concentrations at 0.5 and 1 rpm were similar to other configurations but decreased at higher speeds. At 8 rpm,

Fig. 7. Filter cakes produced from fully submerged HPDR tests: (a) thin cakes (1 to 3 mm) of flocculated copper, (b) thick cake (~20 mm) of non-flocculated copper (83.0 wt%) and (c) thick cake (~20 mm) of flocculated copper (83.1 wt%).

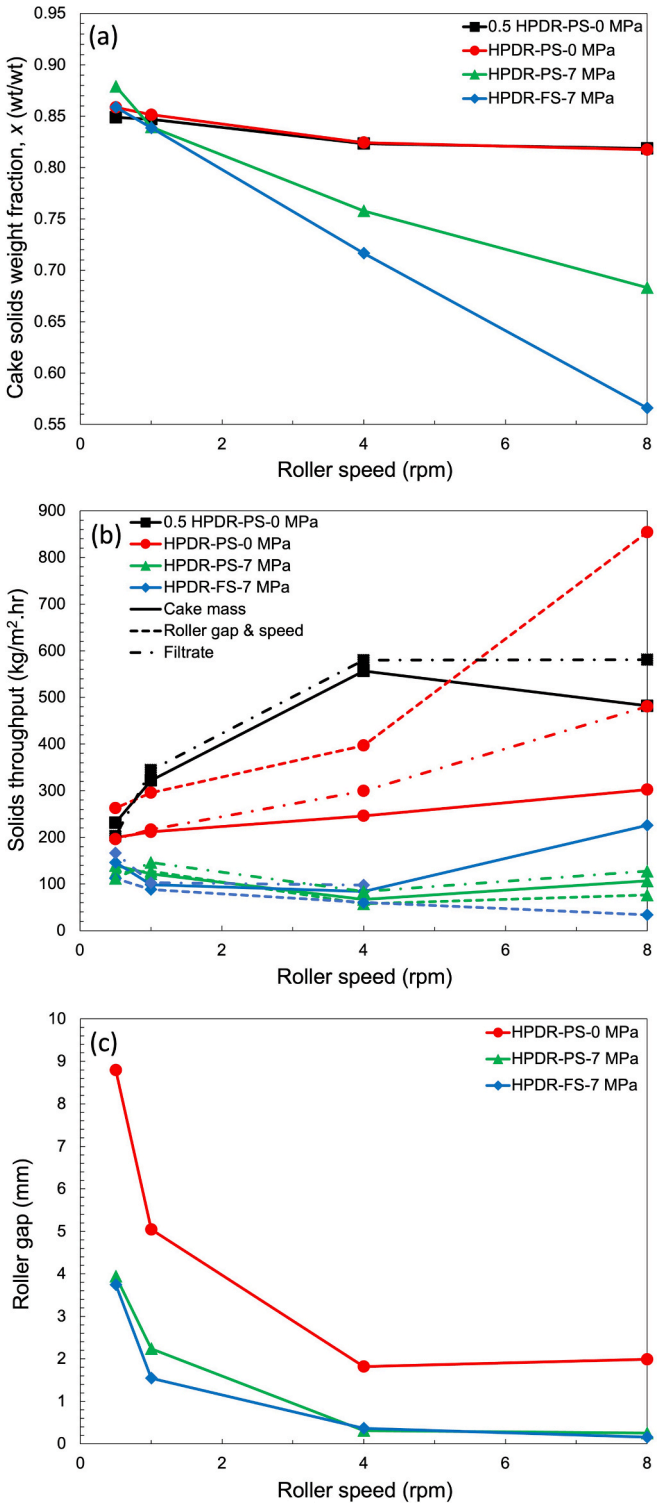

Fig. 8. Effect of varying roller speeds, hydraulics, submersion levels and HPDR arrangements using nickel tailings. All tests were at an initial feed solids concentration of 58 wt%.

leakage from the scraper and cheek plate caused inaccurate throughput measurements. At 4 rpm, some dewatering occurred but was less effective than in the partially submerged tests. Roller gaps were similar to the partially submerged configurations, suggesting material may have floated on the rollers, though it was not visible due to full submersion. Without a desaturation step, cake solids concentration decreased. At 1 rpm, the roller gap was 1.54 mm, yielding 83.9 wt%, while at 0.5 rpm, with a gap of 3.75 mm, the concentration reached 85.9 wt%, comparable to other configurations but lower than in the partially submerged tests, where desaturation improved the concentration.

4.5.2. *Impact on solids throughput*

The three methods to calculate throughput should give the same value if the device is working as expected, and generally do at low rotational rates. If the product chute becomes clogged, the solids throughput calculated by the roller gap and speed method should appear higher than that from the cake mass method, since the clogging restricts material flow but does not affect roller measurements. Additionally, filtrate-based calculations may yield higher throughput estimates than the cake mass method if material floats or product chute clogs, as the suspension may have dewatered but the cake was not collected. Furthermore, any leaks collected in the product bin could lead to an overestimation in the cake mass method.

For the tests without hydraulic pressure, using two rollers was expected to double the throughput. With a single roller, vacuum pressures reached up to −65 kPa, but when both rollers were used, pressures ranged from −43 to −53 kPa. Despite these pressure differences, the final cake solids concentrations remained similar. The reduced throughput (Fig. 8 (b)) can be attributed to the resistance from both the cakes trying to pass through the nip point. A larger vacuum system could potentially achieve higher pressures, though this was not tested.

According to Equation (4), solids throughput is proportional to roller speed, roller gap, and cake solids concentration. In vacuum drum filters without hydraulic pressure, solids throughput calculated by the cake mass method increases with roller speed (Fig. 8 (b)). However, when hydraulic pressure is applied, throughput decreases as roller speed increases due to much reduced roller gap and cake solids concentration (Fig. 8).

At 8 rpm, the solids throughput for HPDR-FS-7 MPa is overestimated because leaks were collected in the product bin. When compared to the roller gap and speed method, which uses Equation (4), the results for configurations with hydraulic pressure closely match the cake mass method. However, the HPDR-PS-0 MPa shows an overestimated throughput due to an exaggerated roller gap in the calculation, caused by the absence of hydraulic pressure, which allows the floating roller to open freely.

In contrast, the filtrate method, which relies on filtrate and mass balance, generally agrees with the other two methods. However, at higher speeds, it tends to indicate a slightly higher throughput due to clogging of the product chute. The dewatered material accumulates in the product chute, causing an overestimation of throughput from the filtrate method since cake is not fully collected in the product bin.

To address the issue of floating material, maintaining a consistent minimum roller gap is crucial. For instance, at 8 rpm with HPDR-PS-0 MPa, the gap widened by 2 mm without hydraulic pressure, forming a 1 mm thick cake on each roller. At 7 MPa pressure, the gap narrowed to 0.25 mm, preventing a 1 mm cake from passing through the nip point, leading to material accumulation on the rollers. To mitigate this, using 2 mm shims between roller housings to maintain a minimum gap of 2 mm is recommended. This ensures optimal cake compression and prevents material from floating. Further optimisation to address these challenges will be explored in future work.

4.5.3. *Effect of shear and initial feed*

Tests were conducted with initial feed solids concentrations of 58.0 wt% and 68.8 wt% under partial submersion and 7 MPa hydraulic pressure. In both cases, cake solids concentration decreased as the roller speed increased. However, higher initial feed concentrations consistently produced higher final cake solids concentrations at the same roller speed (Fig. 10 (a)). The roller gaps remained similar across both feed concentrations (Fig. 10 (c)).

The first two throughput calculation methods, based on cake mass, and roller gap and speed, yielded comparable solids throughput values

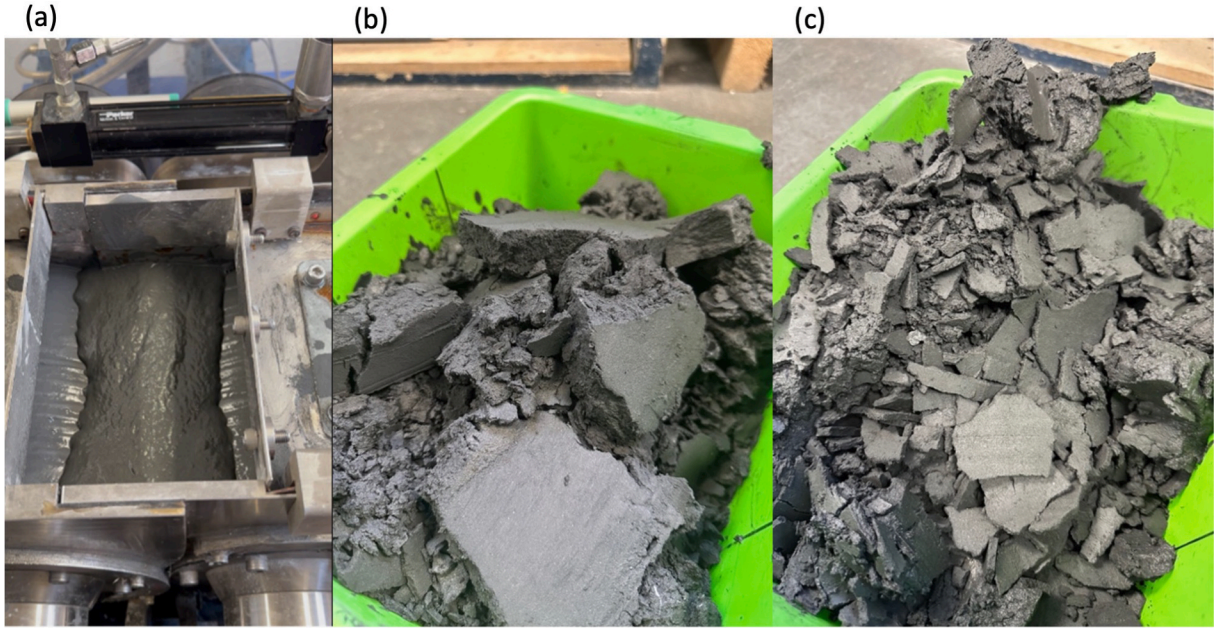

Fig. 9. Partially submerged HPDR tests with nickel tailings under 7 MPa of hydraulic pressure. Suspension floats at 4 rpm (a). No suspension floating at 1 rpm and 0.5 rpm. Cake chunks obtained at 1 rpm (b) and thin sheets of cake were obtained at 0.5 rpm (c).

(Fig. 10 (b)). Maximum throughput occurred at 1 rpm for the 68.8 wt% feed concentration, after which throughput declined due to reduced roller gaps and lower cake solids concentrations.

When compared to the filtrate throughput calculation method, which uses filtrate collection and mass balance, solids throughput was higher, especially at higher speeds, corresponding with observed material floating. The high hydraulic pressure prevented the partially dewatered cake formed on the rollers (using vacuum) from passing through the nip point, causing the material to float on top of the rollers.

Shear application at a 5 % differential roller speed (shear rate of 0.09 s^{-1}) improved the cake solids concentration, but gains diminished at higher shear rates (Fig. 10 (d)). The highest concentration of 88.2 wt% was achieved with a 68.8 wt% feed concentration at a shear rate of 0.09 s^{-1}. However, since these tests were performed at an average roller speed of 0.5 rpm, which already gives very high cake solids concentration, the effect of shear was minimal. Testing in a permeability-limited scenario, such as at higher roller speeds, would likely provide larger differences.

Roller gaps remained relatively consistent across shear rates (Fig. 10 (f)), and the 68.8 wt% feed consistently showed higher solids throughput than the 59.1 wt% feed at all shear rates (Fig. 10 (e)). Throughput does not decrease significantly as shear rates increase (Fig. 10 (e)). While the first two methods showed similar throughput, the filtrate method deviated due to material floating issues.

4.6. Filtration area and solids throughput

The HPDR wedge wire screens, measuring 200 mm in length and 215 mm in diameter, offer a combined surface area of 0.27 m^2 for the two rollers. Laboratory testing with nickel tailings, using the cake mass method, achieved a maximum specific solids throughput of 557 kg/m^2.hr for a single roller. When both rollers were used, the throughput reached a maximum of 302 kg/m^2.hr with a cake solids concentration of 81.7 %. For copper tailings, the filtrate mass method yielded a throughput of 73 kg/m^2.hr with 83.0 % cake solids.

A comparison of performance between the HPDR and filter presses was conducted for processing 5,000 tonnes per day of solids. For nickel tailings, filter press modelling (Stickland et al., 2006) using a fill pressure of 1 MPa and a handling time of 5 min resulted in a specific solids throughput of 281 kg/m^2.hr, requiring 741 m^2 of filtration area to achieve 81.7 % (Table 4). For the nickel tailings, the filtration time was very quick such that the filter press throughput was dominated by the handling time. Extending the handling time to 8 min reduced throughput to 179 kg/m^2.hr and increased the filtration area requirement to 1,165 m^2. In contrast, the HPDR achieved a higher throughput of 302 kg/m^2.hr at the same 81.7 % cake solids, requiring only 690 m^2 of filtration area to process 5,000 tpd.

For copper tailings, the HPDR, operating at its slowest roller speed of 0.44 rpm and without optimisation, produced cake at 83.0 % with a solids throughput of 73 kg/m^2.hr, giving a corresponding filtration area of 2,854 m^2 to process 5000 tpd. 83.0 % is higher than the compressibility of the material at 1 MPa, such that a filter press operating at 1 MPa will never achieve this result. Instead, arbitrarily setting the final average cake concentration at 82.0 % gave a specific solids throughput of 109 kg/m^2.hr, requiring 1,918 m^2 of filtration area to process 5,000 tpd.

In both the copper and nickel tailings, the HPDR achieved concentrations comparable or better than filter presses at similar throughputs per unit filtration area. A concept design for a full-scale HPDR with a diameter of 1.8 m and a length of 7 m, based on dimensions similar to large vacuum drum filters, would provide a roller surface area of 79.2 m^2. This is significantly smaller than the largest filter presses like the GHT5000F Domino, with an area of 2,850 m^2 (Diemme Filtration, 2022), or the Andritz A4F, which offers between 1,400 and 2,100 m^2 (Andritz, 2021).

Despite its advantages, the design of the HPDR inherently provides a lower filtration area per footprint, limiting its feasibility for large-scale operations as it would require many units compared to large filter presses. This indicates that ideal HPDR applications are those that are especially hard to dewater (high fines or clays content), at smaller throughputs, or those that prioritise high solids concentration over throughput, such as copper concentrates.

4.7. Filtrate analysis

The 30 μm gaps in the wedge wire screens physically prevented particles larger than 30 μm from passing through to the filtrate unless they had a high aspect ratio. This was likely to happen immediately after

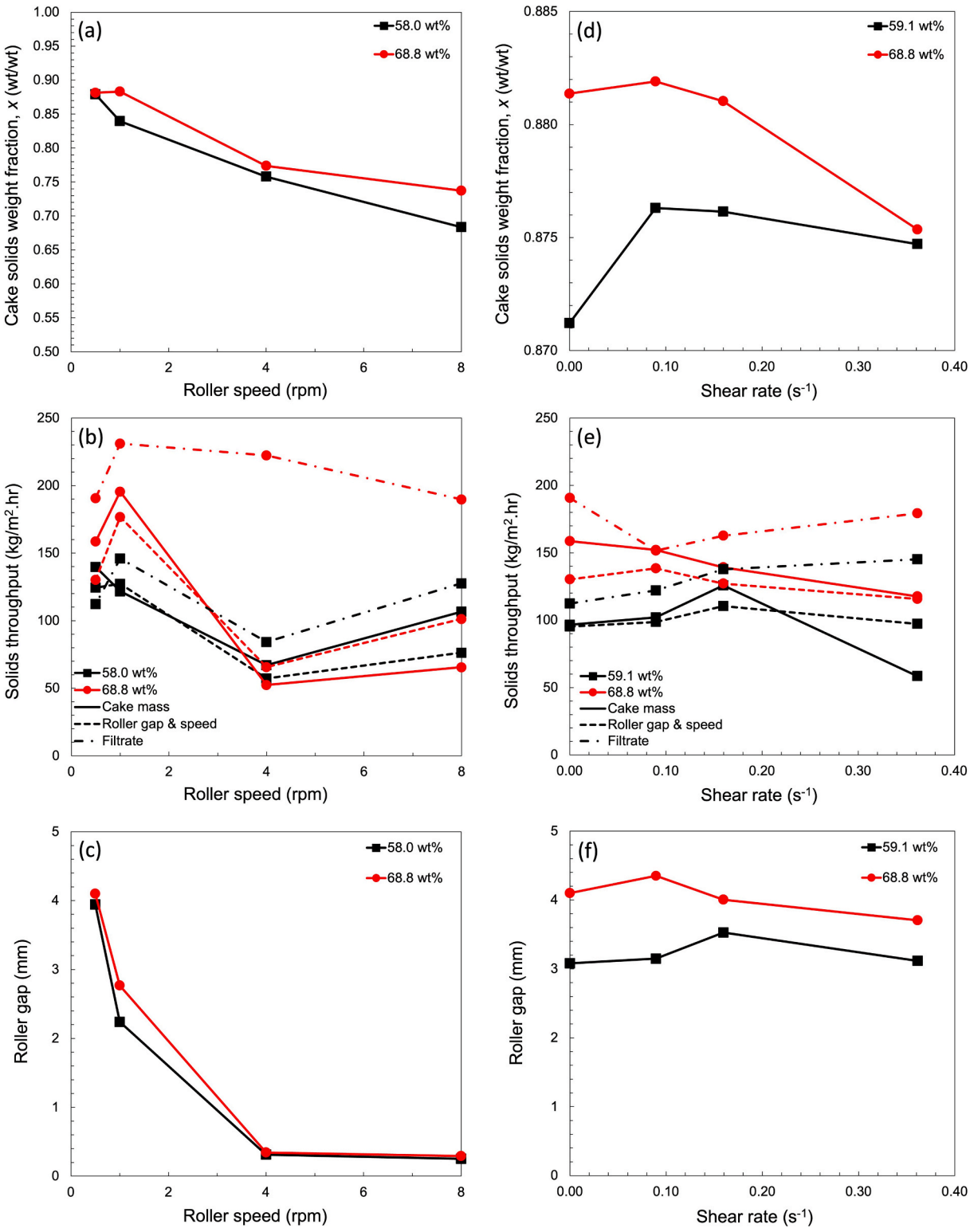

Fig. 10. (a-c) Effects of varying roller speeds and initial feed solids concentrations on nickel tailings. (d-f) Effect of shear and initial feed solids concentrations at an average roller speed of 0.5 rpm. All tests were partially submerged with 7 MPa of hydraulic pressure.

the scrapers, but once a cake formed, the cake itself was expected to capture particles smaller than 30 μm.

In fully submerged tests with the copper tailings, non-flocculated runs resulted in a filtrate suspended solids concentration of 3.1 wt%, decreasing to 2.7 wt% with flocculated tailings, indicating that significant amounts of solids were ending up in the filtrate (Table 5). The d_{90} particle size was less than 30 μm, indicating that there were no defects in the wedge wire as it was stopping nearly all particles greater than 30 μm. The relatively high filtrate concentration is likely due to the start-up phase, where particles could penetrate the wedge wire before a sufficient cake layer formed. Over extended runs, it is expected that the filtrate suspended solids concentration would stabilise as cake resistance increases. To enhance real-time filtrate sampling in next stage feasibility assessment, a second vacuum pump and drum are recommended to

Table 4
Comparison of specific solids throughput and filtration area requirements for nickel and copper tailings based on filter press modelling using material characterisation (Stickland et al., 2006) and lab-scale HPDR test results. Filter press parameters include a 1,000 kPa fill pressure, 5 min of handling time, and negligible membrane resistance.

	Nickel tailings		Copper tailings	
	Filter press	HPDR	Filter press	HPDR
Feed solids concentration (wt%)	58.0	58.0	55.0	55.0
Cake solids concentration (wt%)	81.7	81.7	82.0	83.0
Specific solids throughput (kg/m^{2}hr)	281	302	109	73
Area required for 5,000 tonnes/day (m^2)	741	690	1918	2854

Table 5
Filtrate suspended solids concentration and particle size results for non-flocculated and flocculated copper tailings.

Parameter	Non-flocculated	Flocculated
Solids (wt%)	3.1	2.7
Specific Surface Area (m^2/kg)	1342	1260
D[3,2] (μm)	4.47	4.76
D[4,3] (μm)	10.5	12.6
d_{10}(μm)	2.11	2.21
d_{50}(μm)	6.90	7.35
d_{90}(μm)	22.8	29.4

allow sampling while maintaining vacuum pressure.

For the nickel tailings, the average filtrate suspended solids concentration was 4.7 wt%, largely due to multiple start-up phases during testing at different speeds, allowing particles to pass before the cake layer formed. The PSD remained consistent, with an average D[3,2] of 5.13 μm and d_{50} of 11.9 μm. Approximately 43 % of the feed nickel tailings particles were smaller than 30 μm (Table 3), and only a few larger particles passed through the wedge wire, likely due to their non-spherical shapes. For example, the micrograph of the particles (Fig. 3 (b)) shows a long rod-shaped particle in the top left corner, which has a high aspect ratio and could pass through the wedge wire gap at 30 μm but still measure larger in laser diffraction.

Another contributing factor could be the deterioration of the wedge wires over time, which may allow larger particles to pass. After several months, the HPDR was disassembled, and the wedge wire screens were replaced. There were some dents from earlier tests, but it was unclear if these caused increased solids in the filtrate. When the nickel tailings were used again with new screens, the filtrate PSD results were similar to the average, as shown in Table 6. This suggests that the coarser particle presence in the filtrate were likely caused by particle shape and the non-flocculated feed rather than damage to the wedge wire.

Table 6
Filtrate results summary of nickel tailings.

Parameter	Exp 01	Exp 02	Exp 03	Exp 04	Exp 05 + 06	Average	New Screens
Solids (wt%)	3.6	5.8	5.5	6.5	2.3	4.7	3.0
Specific Surface Area (m^2/kg)	–	1168	1130	1145	1248	1173	1106
D[3,2] (μm)	–	5.14	5.31	5.24	4.81	5.13	5.43
D[4,3] (μm)	–	21.8	24.1	25.0	17.8	22.2	21.6
d_{10} (μm)	–	1.97	2.01	1.99	1.86	1.96	2.10
d_{50} (μm)	–	11.7	12.8	12.4	10.5	11.9	12.5
d_{90} (μm)	–	54.9	62.6	63.9	43.5	56.2	53.3

4.8. Geotechnical tests for filter cake

Geotechnical tests were performed on HPDR cakes. Since both flocculated and non-flocculated copper tailings yielded similar results, the cakes were combined to increase the sample size, resulting in an average dry basis moisture content (MC_d) of 20.9 wt% for UCS tests. For nickel tailings, cakes from runs at 0.5 and 1 rpm from different HPDR arrangements were mixed, yielding an average MC_d of 17.0 wt%.

According to ASTM standards, shear strength is typically half of the compressive strength at failure. In UCS tests, the copper tailings exhibited average strengths of 46.9 kPa (UCS) and 23.5 kPa (shear), while the nickel tailings showed slightly lower values, with an average UCS of 42.7 kPa and shear strength of 21.4 kPa.

Atterberg limit tests revealed liquid limits of 27.3 wt% for the copper and 24.5 wt% for the nickel tailings, with plastic limits of 16.2 wt% and 12.5 wt%, respectively (Table 7). When cake moisture content falls below the liquid limit, the cake ceases to flow like a liquid as shear strength increases and flow resistance develops.

The highest cake solids concentrations were 83.1 wt% for copper and 87.9 wt% for nickel, translating to MC_d values of 20.0 % and 13.6 %, respectively (Table 7). These values surpass the liquid limit, indicating plastic behaviour. The plasticity index for both tailings was similar (11–12 wt%). The cakes from the nickel tailings approached the plastic limit due to a lower breakthrough pressure (17.5 kPa), whereas the cakes from the copper tailings, with a higher breakthrough pressure (302.5 kPa), remained further from desaturation. Applying air pressure above 302.5 kPa could potentially improve the properties of the cakes from the copper tailings.

5. Conclusions

The HPDR Mk-II is a novel solid–liquid separation device specifically designed to address the challenges of dewatering mineral tailings, particularly those with fine particles. It improves upon its predecessor, the Mk-I, by successfully mounting wedge wire screens with fine apertures onto the rolls and increasing the available filtration area. Phase 1 of the study demonstrated the proof-of-concept for the HPDR Mk-II using both flocculated and non-flocculated copper tailings, achieving up to 83.1 wt% solids with fully submerged rollers and high pressures, comparable to conventional filter presses, even under non-optimised conditions.

Several mechanical and design issues were identified in Phase 1, prompting modifications that improved the operational efficiency of the device. The modified HPDR Mk-II successfully demonstrated continuous operation for over an hour with steady feed and cake collection. In Phase 2, nickel tailings were tested under various conditions, and the HPDR Mk-II achieved up to 87.9 wt% solids at 7 MPa hydraulic pressure, exceeding the predicted performance of a conventional filter presses of 85.0 wt% solids at 1 MPa. The air breakthrough pressure of 17.5 kPa for the nickel tailings indicated that the HPDR could be effective as a vacuum drum filter without hydraulic pressure. When operated as a vacuum

Table 7
Atterberg test limits.

	Blend of non-flocculated and flocculated copper HPDR cake	Nickel HPDR cake
Highest HPDR cake moisture content (MC_w wt%)	16.9	12.1
Highest HPDR cake moisture content (MC_d wt%)	20.0	13.6
Liquid limit moisture content (MC_d wt%)	27.3	24.5
Plastic limit moisture content (MC_d wt%)	16.2	12.5
Plasticity index (LL-PL) (MC_d wt%)	11.1	12.0

drum filter, the HPDR produced 84.9 wt% solids, and, when using two vacuum drum filters (with a nip between them), it achieved 85.9 wt% solids. These vacuum configurations exhibited higher throughput due to easier cake transfer into the nip in the absence of hydraulic pressure.

Testing revealed that increased roller speeds in the absence of hydraulic pressure resulted in lower solids concentration but higher throughput. However, high roller speeds with added hydraulic pressure caused material to float above the nip, reducing throughput. Higher feed solids concentrations generally led to improved cake solids concentration and throughput. Partial roller submersion enhanced desaturation effects for the nickel tailings, which full submersion could not achieve, while maintaining consistent throughput across different roller speeds. The application of shear at low speeds had little impact on solids concentration as, in the test conditions, the solids were already close to the compression limit. Further testing on compressible materials in permeability-limited scenarios (i.e. higher roller speeds) may reveal increased benefits of shear.

To address material floating, a mechanism to control the roller gap may be necessary, distinct from the current fixed pressure / floating gap arrangement. Additionally, if slip between the cake and rollers is an issue, varying the roller diameter could yield different results, which warrants further investigation beyond the scope of this work.

In summary, the HPDR Mk-II offers significant advantages over filter presses as a continuous process, with no filter cloths, capable of achieving high solids concentrations and specific throughput, potentially reducing operating and capital costs. For coarser materials and those with lower breakthrough pressures, like the nickel tailings utilised herein, the HPDR can be operated in a vacuum drum configuration. However, the ability of the HPDR Mk-II to provide additional compression through variable hydraulics and deal with tailings incompatible with conventional drum filtration provides great flexibility for a wide range of feed materials with the ability to enhance the dewatering process, improve water recovery, and contribute to more geotechnically stable tailings storage.

CRediT authorship contribution statement

Sajid Hassan: Writing – original draft, Project administration, Methodology, Investigation, Formal analysis. **Raul Cavalida:** Resources, Investigation. **Nilanka I.K. Ekanayake:** Investigation. **Peter J. Scales:** Writing – review & editing, Supervision, Funding acquisition, Conceptualization. **Robin J. Batterham:** Writing – review & editing, Supervision, Funding acquisition, Conceptualization. **Anthony D. Stickland:** Writing – review & editing, Supervision, Resources, Project administration, Methodology, Funding acquisition, Conceptualization.

Declaration of competing interest

The authors declare that they have no known competing financial interests or personal relationships that could have appeared to influence the work reported in this paper.

Acknowledgements

S Hassan is a recipient of the Research Training Program Scholarship from the University of Melbourne, and this project is funded by the Australian Research Council for the ARC Centre of Excellence for Enabling Eco-Efficient Beneficiation of Minerals, grant number CE200100009. The authors extend their sincere thanks to Tony Tran from BHP for supplying the tailings, Deakin University (Melbourne) for conducting the geotechnical tests on the copper tailings, and Mark Coghill from Rio Tinto for his valuable feedback on this paper.

Data availability

Data will be made available on request.

References

Adewuyi, S.O., Anani, A., Luxbacher, K., 2024. Advancing sustainable and circular mining through solid-liquid recovery of mine tailings. Process Saf. Environ. Prot. 189, 31–46.

Andritz, 2021. Excellence in filtration even under roughest conditions. Andritz overhead and sidebar filter presses for mining and minerals [Online]. Available: https://www.andritz.com/resource/blob/422552/aae1871f63f2250ce50d65269e45e754/pas-fp-mining-minerals-en-13-web-data.pdf [Accessed 16th July 2024].

Boger, D.V., Scales, P.J. Sofra, F., 2006. Rheological Concepts. Chapter 3 in Paste and thickened tailings: A Guide for Industry. Second Edition, Nedlands, W.A, Australian Centre for Geomechanics.

Buscall, R., White, L.R., 1987. The consolidation of concentrated suspensions. Part 1.—The theory of sedimentation. J. Chem. Soc. Faraday Trans. 1 83, 873–891.

Chaedir, B.A., Kurnia, J.C., Sasmito, A.P., Mujumdar, A.S., 2021. Advances in dewatering and drying in mineral processing. Drying Technol. 39, 1667–1684.

Chen, C., 2022. Hazards identification and characterisation of the tailings storage facility dam failure and engineering applications. Int. J. Min. Reclam. Environ. 36, 399–418.

Chen, G., Lock Yue, P., Mujumdar, A.S., 2002. Sludge dewatering and drying. Drying Technol. 20, 883–916.

Concha, F. 2014. Solid-Liquid Separation in the Mining Industry. Fluid Mechanics and Its Application Series, ISBN 978-3-319-02483-7.

De Kretser, R.G., Usher, S.P., Scales, P.J., Boger, D.V., Landman, K.A., 2001. Rapid filtration measurement of dewatering design and optimization parameters. AIChE J 47, 1758–1769.

Diemme Filtration. 2022. *GHT5000F Domino* [Online]. Available: https://www.diemmefiltration.com/filterpress-for-sludge/filter-press-ght-5000f-domino/ [Accessed 5th Feb 2024].

Fisher, D.T., Clayton, S.A., Boger, D.V., Scales, P.J., 2007. The bucket rheometer for shear stress-shear rate measurement of industrial suspensions. J. Rheol. 51, 821–831.

Furnell, E., Bilaniuk, K., Goldbaum, M., Shoaib, M., Wani, O., Tian, X., Chen, Z., Boucher, D., Bobicki, E.R., 2022. Dewatered and stacked mine tailings: a review. ACS ES&T Eng. 2, 728–745.

Gauthier, F.G.R., Danforth, S.C., 1991. Packing of bimodal mixtures of colloidal silica. J. Mater. Sci. 26, 6035–6043.

Gleiss, M., Nirschl, H., 2015. Modeling separation processes in decanter centrifuges by considering the sediment build-up. Chem. Eng. Technol. 38, 1873–1882.

Green, M.D., Landman, K.A., De Kretser, R.G., Boger, D.V., 1998. Pressure filtration technique for complete characterization of consolidating suspensions. Ind. Eng. Chem. Res. 37, 4152–4156.

Haldar, S.K., 2018. Chapter 13 - Mineral Processing. In: HALDAR, S. K. (ed.) Mineral Exploration (Second Edition). Elsevier.

Hammerich, S., Stickland, A.D., Radel, B., Gleiss, M., Nirschl, H., 2020. Modified shear cell for characterization of the rheological behavior of particulate networks under compression. Particuology 51, 1–9.

Hamraoui, L., Bergani, A., Ettoumi, M., Aboulaich, A., Taha, Y., Khalil, A., Neculita, C. M., Benzaazoua, M., 2024. Towards a circular economy in the mining industry: possible solutions for water recovery through advanced mineral tailings dewatering. Minerals 14, 319.

Haramkar, S.S., Thombre, G.N., Jadhav, S.V., Thorat, B.N., 2021. The influence of particle(s) size, shape and distribution on cake filtration mechanics—a short review. C. R. Chim. 24, 255–265.

Hassan, S., Ekanayake, N.I.K., Scales, P.J., Batterham, R.J., Stickland, A.D., 2023. High pressure dewatering rolls Mk-II: a novel dewatering technology for mineral tailings. FILTECH 2023 Conference Proceedings. Cologne, Germany.

Höfgen, E., Collini, D., Batterham, R.J., Scales, P.J., Stickland, A.D., 2019. High pressure dewatering rolls: comparison of a novel prototype to existing industrial technology. Chem. Eng. Sci. 205, 106–120.

Höfgen, E., Teo, H.-E., Scales, P.J., Stickland, A.D., 2020. Vane-in-a-filter and vane-under-compressional-loading: novel methods for the characterisation of combined shear and compression. Rheol. Acta 59, 349–363.

Huttunen, M., Nygren, L., Kinnarinen, T., Ekberg, B., Lindh, T., Karvonen, V., Ahola, J., Häkkinen, A., 2019. Real-time monitoring of the moisture content of filter cakes in vacuum filters by a novel soft sensor. Sep. Purif. Technol. 223, 282–291.

Huttunen, M., Nygren, L., Kinnarinen, T., Häkkinen, A., Lindh, T., Ahola, J., Karvonen, V., 2017. Specific energy consumption of cake dewatering with vacuum filters. Miner. Eng. 100, 144–154.

Illies, S., Pfinder, J., Anlauf, H., Nirschl, H., 2017. Filter cake compaction by oscillatory shear. Drying Technol. 35, 66–75.

International Council on Mining and Metals, United Nations Environment Programme & Principles for Responsible Investment 2020. Global Industry Standard on Tailings Management.

Klug, R., Schwarz, N., 2019. Dewatering tailings: rapid water recovery by use of centrifuges. In: Paterson, A.J.C., A.B.F., Reid, D., (eds.) Paste 2019: Proceedings of the 22nd International Conference on Paste, Thickened and Filtered Tailings. Cape Town: Australian Centre for Geomechanics.

Lester, D.R., Usher, S., Scales, P.J., 2005. Estimation of the hindered settling function R (ϕ) from batch settling tests. AIChE J 51, 1158–1168.

Menesklou, P., Nirschl, H., Gleiss, M., 2020. Dewatering of finely dispersed calcium carbonate-water slurries in decanter centrifuges: about modelling of a dynamic simulation tool. Sep. Purif. Technol. 251, 117287.

Menesklou, P., Sinn, T., Nirschl, H., Gleiss, M., 2021. Scale-up of decanter centrifuges for the particle separation and mechanical dewatering in the minerals processing industry by means of a numerical process model. Minerals 11, 229.

Merkl, R., Steiger, W., 2012. Properties of decanter centrifuges in the mining industry. Min. Metall. Explor. 29, 6–12.
Nguyen, C.V., Nguyen, A.V., Doi, A., Dinh, E., Nguyen, T.V., Ejtemaei, M., Osborne, D., 2021. Advanced solid-liquid separation for dewatering fine coal tailings by combining chemical reagents and solid bowl centrifugation. Sep. Purif. Technol. 259, 118172.
Queiroz, H.M., Nóbrega, G.N., Ferreira, T.O., Almeida, L.S., Romero, T.B., Santaella, S.T., Bernardino, A.F., Otero, X.L., 2018. The Samarco mine tailing disaster: a possible time-bomb for heavy metals contamination? Sci. Total Environ. 637–638, 498–506.
Reichmann, B., Tomas, J., 2001. Expression behaviour of fine particle suspensions and the consolidated cake strength. Powder Technol. 121, 182–189.
Reif, F., Stahl, W., Langeloh, T., 1990. Optimising decanter centrifuges. Filtr. Sep. 27, 408–410.
Rotta, L.H.S., Alcântara, E., Park, E., Negri, R.G., Lin, Y.N., Bernardo, N., Mendes, T.S.G., Souza Filho, C.R., 2020. The 2019 Brumadinho tailings dam collapse: possible cause and impacts of the worst human and environmental disaster in Brazil. Int. J. Appl. Earth Obs. Geoinf. 90, 102119.
Scales, P.J., Tordesillas, A., Stickland, A.D., Batterham, R.J., 2017a. Improvements in comminution and/or removal of liquid from a material (Chile Patent No. CL2017/001484), Chile Patent Office.
Scales, P.J., Tordesillas, A., Stickland, A.D., Batterham, R.J., 2017b. Separation of liquid from a material, (Australian Patent No. AU 2012/283684 B2), IP Australia.
Simpson, G.D., 1964. Operation of Vacuum Filters. Journal (Water Pollution Control Federation), 36, 1460-1467.
Stickland, A.D., Batterham, R.J., Scales, P.J., 2024. An apparatus for dewatering a suspension. Patent Number: WO2025/065052.
Stickland, A.D., De Kretser, R.G., Scales, P.J., Usher, S.P., Hillis, P., Tillotson, M.R., 2006. Numerical modelling of fixed-cavity plate-and-frame filtration: Formulation, validation and optimisation. Chem. Eng. Sci. 61, 3818–3829.
Stickland, A.D., Teo, H.-E., Franks, G.V., Scales, P.J., 2014. Compressive strength and capillary pressure: competing properties of particulate suspensions that determine the onset of desaturation. Drying Technol. 32, 1614–1620.
Stickland, A.D., White, L.R., Scales, P.J., 2011. Models of rotary vacuum drum and disc filters for flocculated suspensions. AIChE J 57, 951–961.
Sung, D.-J., Turian, R.M., 1994. Chemically enhanced filtration and dewatering of narrow-sized coal particles. Sep. Technol. 4, 130–143.
Svarovsky, L. 2001. 13 - Vacuum filtration. In: SVAROVSKY, L. (ed.) Solid-Liquid Separation (Fourth Edition). Oxford: Butterworth-Heinemann.
Usher, S.P., De Kretser, R.G., Scales, P.J., 2001. Validation of a new filtration technique for dewaterability characterisation. AIChE J 47, 1561–1570.
Usher, S.P., Studer, L.J., Wall, R.C., Scales, P.J., 2013. Characterisation of dewaterability from equilibrium and transient centrifugation test data. Chem. Eng. Sci. 93, 277–291.
Vaxelaire, J., Olivier, J., 2006. Conditioning for municipal sludge dewatering. From filtration compression cell tests to belt press. Drying Technol. 24, 1225–1233.
Vaxelaire, J., Olivier, J., 2014. Compression dewatering of particulate suspensions and sludge: effect of Shear. Drying Technol. 32, 23–29.
Wakeman, R.J., 2007. Separation technologies for sludge dewatering. J. Hazard. Mater. 144, 614–619.
Wang, C., Harbottle, D., Liu, Q., Xu, Z., 2014. Current state of fine mineral tailings treatment: a critical review on theory and practice. Miner. Eng. 58, 113–131.
Williams, D.J., 2021. Lessons from tailings dam failures—where to go from here? Minerals 11, 853.
Zhou, Z., Scales, P.J., Boger, D.V., 2001. Chemical and physical control of the rheology of concentrated metal oxide suspensions. Chem. Eng. Sci. 56, 2901–2920.